Bioactive Materials 26 (2023) 52–63

Contents lists available at ScienceDirect

Bioactive Materials

journal homepage: www.keaipublishing.com/en/journals/bioactive-materials

Targeted PERK inhibition with biomimetic nanoclusters confers preventative and interventional benefits to elastase-induced abdominal aortic aneurysms

Nisakorn Yodsanit [a,b,1], Takuro Shirasu [c,1], Yitao Huang [c,d,1], Li Yin [c], Zain Husain Islam [c], Alexander Christopher Gregg [c], Alessandra Marie Riccio [c], Runze Tang [c], Eric William Kent [c], Yuyuan Wang [a,b], Ruosen Xie [a,b], Yi Zhao [a,b], Mingzhou Ye [a,b], Jingcheng Zhu [a,b], Yi Huang [e], Nicholas Hoyt [c,f], Mengxue Zhang [c], John A. Hossack [e], Morgan Salmon [g], K. Craig Kent [c], Lian-Wang Guo [c,**], Shaoqin Gong [a,b,*], Bowen Wang [c,***]

[a] Department of Biomedical Engineering, Wisconsin Institute for Discovery, University of Wisconsin-Madison, Madison, WI, 53715, USA
[b] Department of Ophthalmology and Visual Sciences, University of Wisconsin-Madison, Madison, WI, 53715, USA
[c] Department of Surgery, School of Medicine, University of Virginia, Charlottesville, VA, 22908, USA
[d] The Biomedical Sciences Graduate Program (BIMS), School of Medicine, University of Virginia, Charlottesville, VA, 22908, USA
[e] Department of Biomedical Engineering, School of Engineering, University of Virginia, Charlottesville, VA, 22908, USA
[f] School of Medicine and Health Sciences, George Washington University, Washington, DC, 20052, USA
[g] Department of Cardiac Surgery, Michigan Medicine, University of Michigan, Ann Arbor, MI, 48109, USA

ARTICLE INFO

Keywords:
Abdominal aortic aneurysm
ER stress
PERK
Biomimetic nanomedicine
Targeted delivery

ABSTRACT

Abdominal aortic aneurysm (AAA) is a progressive aortic dilatation, causing ~80% mortality upon rupture. Currently, there is no approved drug therapy for AAA. Surgical repairs are invasive and risky and thus not recommended to patients with small AAAs which, however, account for ~90% of the newly diagnosed cases. It is therefore a compelling unmet clinical need to discover effective non-invasive strategies to prevent or slow down AAA progression. We contend that the first AAA drug therapy will only arise through discoveries of both effective drug targets and innovative delivery methods. There is substantial evidence that degenerative smooth muscle cells (SMCs) orchestrate AAA pathogenesis and progression. In this study, we made an exciting finding that PERK, the endoplasmic reticulum (ER) stress Protein Kinase R-like ER Kinase, is a potent driver of SMC degeneration and hence a potential therapeutic target. Indeed, local knockdown of PERK in elastase-challenged aorta significantly attenuated AAA lesions in vivo. In parallel, we also conceived a biomimetic nanocluster (NC) design uniquely tailored to AAA-targeting drug delivery. This NC demonstrated excellent AAA homing via a platelet-derived biomembrane coating; and when loaded with a selective PERK inhibitor (PERKi, GSK2656157), the NC therapy conferred remarkable benefits in both preventing aneurysm development and halting the progression of pre-existing aneurysmal lesions in two distinct rodent models of AAA. In summary, our current study not only establishes a new intervention target for mitigating SMC degeneration and aneurysmal pathogenesis, but also provides a powerful tool to facilitate the development of effective drug therapy of AAA.

Peer review under responsibility of KeAi Communications Co., Ltd.
* Corresponding author. Department of Biomedical Engineering, Wisconsin Institute for Discovery, University of Wisconsin-Madison, Madison, WI, 53715, USA.
** Corresponding author.
*** Corresponding author.
E-mail address: shaoqingong@wisc.edu (S. Gong).
[1] Equal contributions.

https://doi.org/10.1016/j.bioactmat.2023.02.009
Received 19 April 2022; Received in revised form 8 February 2023; Accepted 8 February 2023

1. Introduction

Abdominal aortic aneurysm (AAA) is a common and highly lethal type of vascular disease, claiming an estimated total number of 13,000 deaths per year in the US alone [1,2]. AAA features progressive weakening and dilation of the abdominal aortic wall culminating in the abrupt and lethal rupture which is associated with an 80% mortality rate [2,3]. Unfortunately, despite the recent progress in AAA screening, there is still no medical treatment that can effectively prevent or halt the expansion and rupture of AAA lesions [4,5]. Surgical repairs remain the only option available in the clinic for management of AAA, which can be not only costly and risky, but also leaves patients with small diameter AAA lesions on "watchful waiting" with no treatment [6,7]. Therefore, it is imperative to develop effective non-surgical strategies to fulfil this unmet clinical need [8].

The current lack of a pharmacological therapy for AAA can be partly attributed to our incomplete understanding of this disease. The etiology of AAA is multifactorial [9]. While the contribution from circulating factors has long been considered critical to AAA pathophysiology [10–12], recent studies start to shed new light on the importance of vascular smooth muscle cells (SMCs) in AAA formation and rupture [13–16]. Indeed, SMCs are the most prevalent cell type that constitutes the mechanical strength and elasticity of the aortic wall [17]. Under diseased conditions, SMCs can display a wide range of degenerative phenotypes that directly contribute to the aortic destruction, including cell death, pro-inflammatory and proteolytic behaviors [15,18]. Therefore, understanding and targeting SMC degeneration may hold the key to developing effective medical treatments for AAA.

Another key roadblock to AAA therapy is the lack of targeted drug delivery. With a traditional route of systemic delivery approach, low drug doses are often ineffective yet high doses are too toxic – a dilemma epitomized by doxycycline, a once promising AAA drug that has underwent two decades of active clinical trials yet recently deemed ineffective [4,5,19]. The advent of nanotechnology offers a promising solution to improve the formulation of existing and investigative drugs, with demonstrated success in clinical applications such as chemotherapy and vaccine development [20,21]. However, as summarized in our recent review, the paucity of published reports on developing AAA-targeting nanoparticles testifies the need for further research efforts on this pressing topic [22].

We envision that translational success requires the discovery of an effective intervention target (new drug) coupled with precision drug delivery (new nanoplatform) to the AAA lesion. In this study, we present experimental evidence supporting the role of protein kinase RNA-like endoplasmic reticulum kinase (PERK) in driving SMC degeneration and hence AAA pathogenesis. PERK represents one of the three branches of the endoplasmic reticulum (ER) stress response pathway tightly involved in multiple vascular diseases, yet its mechanistic and therapeutic implications in aneurysms remain largely unknown. In parallel, we developed a nanoparticle platform for the targeted delivery of GSK2656157, a second-generation selective inhibitor of PERK [23]. Coated with platelet membranes, the nanoclusters (NC) —composed of dendritic poly(amidoamine) (PAMAM)-poly(lactic-*co*-glycolic acid) (PLGA) nanoparticles— displayed selective lesion-targeting capacity at different stages of elastase-induced experimental AAA.

Finally, our study demonstrated both preventive and interventional value of targeted PERK inhibition therapies, as a weekly regimen of GSK2656157-loaded biomimetic NC can effectively block the aneurysmal dilation in rodents with either acutely injured aortas or pre-existing AAA lesions.

2. Materials and methods

2.1. Materials

Dendritic poly(amidoamine) (PAMAM) (4^{th} generation with hydroxyl terminal), dimethyl sulfoxide (DMSO), glycolide, lactide, and tin(II) 2-ethylhexanoate ($Sn(Oct)_2$) were acquired from Sigma-Aldrich (St. Louis, MO). PERK inhibitor (PERKi, GSK2656157) was purchased from LC laboratories (Woburn, MA). Cyanine5 (Cy5) fluorescent dye was obtained from Lumiprobe Co. (Hallandale Beach, FL). Other reagents were purchased from Thermo Fisher Scientific (Fitchburg, WI).

2.2. Preparation and characterization of the biomimetic nanoclusters (NC)

First, PAMAM, glycolide and lactide were used to synthesize PAMAM-PLGA-OH *via* ring-opening polymerization using $Sn(Oct)_2$ as a catalyst [24]. PAMAM-PLGA-OH was then reacted with succinic anhydride under basic pH to yield PAMAM-PLGA-COOH [25]. Cy5 was conjugated onto the surface of PAMAM-PLGA-COOH through an amidation reaction to yield fluorescent PAMAM-PLGA-COOH/Cy5 [25]. The chemical structures of PAMAM-PLGA-OH, PAMAM-PLGA-COOH, and PAMAM-PLGA-COOH/Cy5 were characterized by proton nuclear magnetic resonance spectroscopy (^{1}H NMR) and Fourier-transform infrared (FTIR) spectroscopy. Furthermore, the molecular weight was determined using triple-detection gel permeation chromatography (GPC). The degradation profiles of the PAMAM-PLGA-COOH polymer stored in buffers with a pH value of either 5.5 or 7.4 at 37 °C were quantified by monitoring the weight loss and molecular weight (using GPC) of the polymer for 4 weeks [26,27].

PERKi was loaded into PAMAM-PLGA-COOH via a dialysis method [28,29]. The resulting PERKi-loaded unimolecular nanoparticles were suspended in PBS to form nanoclusters spontaneously. The platelet membrane-coated nanoclusters (aka biomimetic NC) were fabricated via an extrusion process. To validate the successful coating process of platelet membrane on nanocluster, confocal imaging was used to observe the colocalization of Cy5 and DiO which were used to label PAMAM-PLGA-COOH and platelet membrane, respectively [30]. The hydrodynamic diameters, zeta potentials, and morphology of the biomimetic NC were studied by dynamic light scattering (DLS) and transmission electron microscope (TEM). The loading content and release profile of PERKi in the biomimetic NC were quantified by HPLC. Detailed information on the preparation and characterization of the biomimetic NC can be found in the supplementary document and Fig. S1.

2.3. Protocol statement

All animal studies conform to the National Institutes of Health Guide for the Care and Use of Laboratory Animals. Research protocols are approved by the Institutional Animal Care and Use Committees and Institutional Biosafety Committee at University of Virginia. Human specimens were obtained under approved institutional review board (IRB), including tissue slides from de-identified donors provided by CVPath Institute (Gaithersburg, MD).

2.4. Cell culture

Human aortic VSMC and culture media (SmBm-2 basal medium for experimental purposes, and SmGm-2 complete medium for expansion) were purchased from Lonza (Walkersville, MD) and cultured at 37 °C with 5% CO_2 as previously described [31,32]. To ensure the properties of SMC contractile phenotypes, we limited the primary cell culture to passage 5–7 for all the *in vitro* experiments described in this study. Accutase (Thermo Fisher Scientific, Waltham, MA) was used for cell detachment to ensure fast cell adhesion and optimal cell status as established in our prior reports [31,32].

2.5. Elastase-perfusion procedure to create acute AAA in rats

All adult male Sprague-Dawley rats (Charles River, weighing

300–350 g) were maintained in a temperature and humidity-controlled animal facility under a 12 h light-dark cycle. Food and water were available ad libitum. Animals were randomly assigned to each treatment group. Elastase perfusion was performed as previously described [33]. Following confirmation of anesthesia (isoflurane) and sterile preparation of the incision sites, a midline incision was made and the infrarenal region of the abdominal aorta was isolated. The pre-perfusion maximal aortic diameter was recorded using an electric microcaliper. After ligating aortic branches, the aortic diameter before infusion was measured. A PE-10 polyethylene tubing was inserted via right saphenous artery and advanced to the infrarenal region, and temporary ligations were applied to both proximal and distal end of the isolated aorta segment. The infrarenal segment of the abdominal aorta was then continuously perfused with 0.27 mL porcine elastase solution (1 unit/mL) over the course of 54 min using an infusion pump. After the infusion, the tubing was retrieved. After confirming the reperfusion of blood flow and hemostasis, the maximal aortic diameter after infusion was recorded. Bowel contents was recovered, muscle layers were re-approximated with 4-0 nylon sutures, and then a secondary closure was made to close the skin with 4-0 nylon sutures. For the therapeutic studies, rats received intravenous injection of the NC or appropriate control treatment (at the dosage of 2.5 mg/kg) through tail veins immediately post procedure. Localized viral transduction in elastase-perfused rat abdominal aorta was achieved as previously described [34], using lentivirus solution for scrambled or PERK-specific shRNA ($>1 \times 10^9$ IFU/mL) as described and validated in our prior study [31]. Analgesics and post-operative care were provided according to ACUC policy at University of Virginia.

2.6. Murine model with chronic AAA development

A chronic model of AAA was adopted from that described by Guanyi Lu et al. [35] All male c57bl/6 mice (The Jackson Laboratory, 8–12 weeks) were maintained in a temperature and humidity-controlled animal facility under a 12 h light-dark cycle. Mice were subject to drinking water modification with 0.2% β-Aminopropionitrile (BAPN), starting 3 days prior to the elastase challenge. The modified elastase procedure was performed based on a recently published methodology [35]. Following confirmation of anesthesia (isoflurane) and sterile preparation of the incision sites, a midline incision was made and the infrarenal region of the abdominal aorta was dissected. The mice received topical application of 0.2 U porcine pancreatic elastase for 8 min onto the abdominal aortic segment. After removing and rinsing the residual elastase solutions, bowel contents were returned to the original positions, muscle layers were re-approximated with 7-0 nylon ligature, and then a secondary closure was made to close the skin with 7-0 nylon ligature. For the intervention studies, mice received intravenous injection of the NC or appropriate control treatment (at the dosage of 2.5 mg/kg) through tail veins at day 7 post elastase procedure — a time point at which mice developed established AAA lesions as characterized in prior studies [36]. Mice continued to receive weekly injections of the therapeutics or the respective controls through the 4-week course of study. Murine AAA lesions were evaluated based on maximal aortic diameters using Vevo 2100 high-resolution ultrasound imaging at day 0 (baseline), day 7, and day 28, as described in Supplementary Document.

2.7. Histological examination of tissue specimens

After euthanasia, abdominal aortas and the main organs or tissues including heart, liver, lung, spleen, intestine, and kidney were collected, fixed with 4% paraformaldehyde, and embedded in paraffin in a tissue base mold. The paraffin blocks of human or rodent tissues were sectioned at a microtome setting of 5 μm for Hematoxylin&Eosin (H&E), Van Gieson's (VVG), and Masson's trichrome (MT) staining, as well as immunofluorescent staining, as previously described [32,37]. For immunofluorescent staining, antigen retrieval was conducted using a decloaking chamber (NxGen, Biocare Medical, Pacheco, CA), followed by incubation with primary antibodies. Depending on whether dye-conjugated primary antibodies were used, the sections were then incubated with corresponding secondary antibodies conjugated with Alexa Fluor 594 for 1.5hr. Detailed information of antibodies is included in Supplemental Table S1. For frozen sections, unfixed abdominal aortic specimens were embedded in OCT compound (Tissue-Tek, Sakura Finetek). To determine the *in situ* localization of NC and cellular colocalization, frozen sections from mice administered with Cy5-conjugated biomimetic NC were subjected to co-staining with Alexa Fluor-conjugated antibodies for SMC marker (αSMA) and macrophage marker (CD68). The images were captured by an EVOS M7000 microscope for morphometric and epi-fluorescent analysis, or by a STELLARIS 5 confocal point scanning system with Leica DMi8 inverted microscope (Leia Microsystems Inc., Buffalo Grove, IL).

2.8. mRNA extraction, and qPCR analysis

mRNA was isolated from cultured VSMC and collected tissue specimens using TRIzol following the manufacturer's instructions. Purified mRNA (1 μg) was used for the first-strand cDNA synthesis and quantitative RT-PCR was performed using the QuantStudio3 (Applied Biosystems, Carlsbad, CA). Each cDNA template was amplified in triplicates using SYBR Green PCR Master Mix, with the primer sequences provided in the Supplementary Document (Table S2).

2.9. Statistical analysis

All data are presented as mean ± standard error of the mean (SEM). Statistical analysis was performed using GraphPad Prism 9.1.0. For multiple group-wise comparison, one-way analysis of variance (ANOVA) was performed followed by Tukey post-hoc tests. For two-group comparison, Student's t-test was performed. The value $P < 0.05$ was considered to be statistically significant.

3. Results

3.1. The PERK pathway is activated in clinical and experimental AAAs

ER stress PERK pathway represents a promising therapeutic target in vascular diseases, and recent studies suggest a possible correlation between aberrant ER stress response and AAA [38,39]. In the present study, we first determined the level of PERK activation in healthy aorta versus AAA specimens from human donors. As shown in Fig. 1A, immunofluorescence staining revealed excessive phosphorylation of PERK (p-Thr980, P-PERK) in degenerative SMCs (co-staining with SMC marker, αSMA) as well as macrophages (co-staining with macrophage marker, CD68) in aneurysmal aortas collected from AAA patients (note the disrupted smooth muscle content and elastic laminae), and its activation level (determined by P-PERK fluorescence intensity as in Fig. 1B) was significantly higher than that from healthy aortas. Similarly, Western blot analysis of aortic tissue homogenates also revealed significant upregulations of PERK activation (P-PERK) as well as its downstream proteins (ATF4 and CHOP) in elastase-induced experimental AAA specimens from rats (Fig. 1C and D). Of particular note, CHOP is the effector transcription factor shared by all ER stress response pathways and closely implicated in cell death initiation, and recent study revealed that CHOP global deficiency protected against thoracic aortic aneurysm/dissection [40,41]. Collectively, our data confirm the robust activation of PERK pathway in experimental AAA models as well as degenerative, pro-AAA SMCs, and hence suggests a potential role of PERK-targeting agents in AAA treatment.

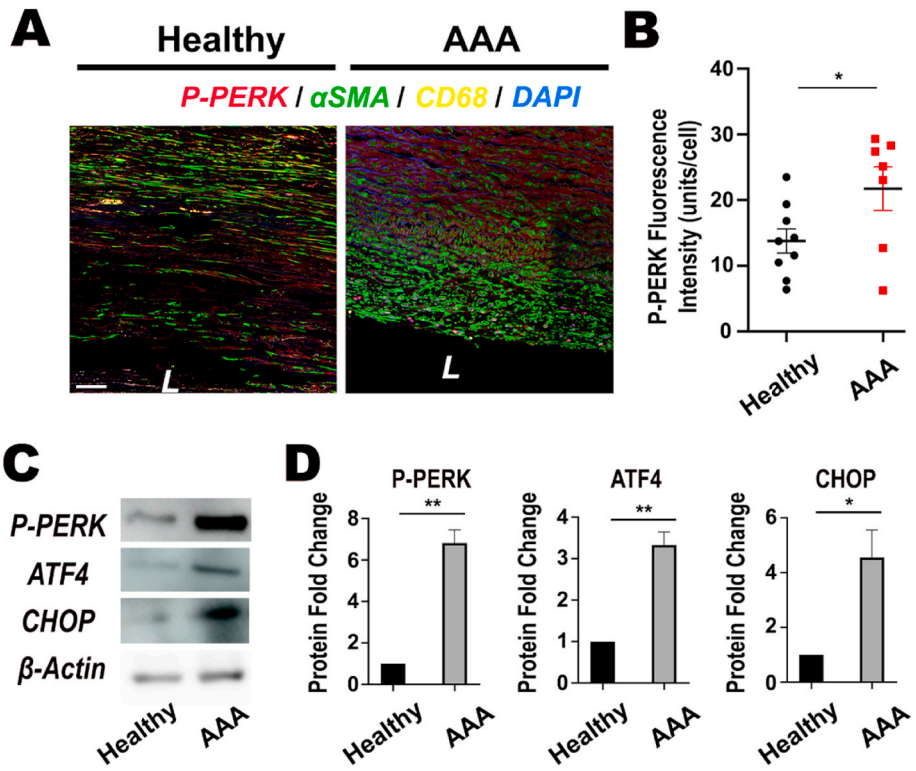

Fig. 1. ***The PERK Pathway is Activated in Clinical and Experimental Specimens of AAA.*** (A) Immunofluorescence co-staining of phospho-PERK (P-PERK, Thr980), SMC marker αSMA, and macrophage marker CD68 on sections of healthy aorta versus AAA lesions from de-identified human donors (note loss of SMC contents in AAA specimens). L: luminal side. (B) Quantification of P-PERK fluorescent intensity in human specimens. Mean ± SEM, n = 7-9. *P < 0.05. Unpaired Student's *t*-test. (C) Representative images of immunoblots for PERK pathway proteins (P-PERK, ATF4, CHOP) using tissue homogenates from healthy rat aorta versus elastase-induced AAA specimens. (D) Quantitation of P-PERK, ATF4, and CHOP levels based on immunoblot densitometry after normalization to β-Actin. Mean ± SEM, n = 4. *P < 0.05, **P < 0.01. Paired Student's *t*-test.

3.2. PERK loss-of-function reverses, its gain-of-function exacerbates SMC Degeneration In Vitro

The degenerative phenotype transition of SMC is the critical step that foreshadows the aneurysmal expansion and the ultimate wall collapse [15,42]. In the current study, we challenged primary culture of human SMC with transient porcine pancreas elastase exposure to induce cell death as established in previous studies [43]; in parallel, TNFα, a classic stimuli of cellular degeneration, was administered to stimulate the pro-inflammatory, proteolytic, and de-differentiated gene responses in SMC [44]. It is worth noting that TNFα stimulation alone is not sufficient to induce SMC death [44]. As shown in Fig. 2, silencing PERK with siRNA effectively rescued the loss of SMC viability and pro-apoptotic Caspase-3/7 activities (Fig. 2A), and in the meanwhile, profoundly reduced the mRNA levels of markers of the pro-inflammatory (IL6, MCP1) and proteolytic responses (MMP2) (Fig. 2B). Consistent with our prior studies, the reduction in PERK expression led to significant restoration of αSMA expression (Fig. 2B), whose reduction upon TNFα stimulation is a known indicator of SMC's de-differentiation. Conversely, adenovirus-mediated PERK overexpression exacerbated SMC death (Fig. 2C and D). Together, these *in vitro* loss- and gain-of-function results strongly support a key role of PERK in driving the degenerative, pro-AAA phenotype transition of SMC.

3.3. Local PERK silencing confers effective control over Development of Elastase-induced AAA lesions

To further establish the role of PERK as a potential intervention target in AAA management, we performed local transgene study in vivo via intraluminal infusion of lentivirus to achieve localized shRNA-mediated knockdown following elastase induction (Fig. 3A). *In situ* macroscopic analysis of abdominal aorta indicates a significantly reduced aortic diameter from animals transduced with PERK-silencing lentivirus, in comparison to the scrambled shRNA control (Fig. 3B and C). Additionally, using tissue mRNA samples from resected aneurysmal lesions, we observed significant amelioration of hallmarks of degenerative SMC phenotype as shown in Fig. 3D, including reduced expression of ECM proteolytic gene MMP2, mitigation of inflammatory response gene IL6, and preservation of smooth muscle content as evidenced by increased αSMA level. Similarly, immunostaining of Myh11 confirmed the successful restoration of SMC differentiation proteins (Fig. S2A). Additionally, MCP1, a potent macrophage chemoattractant critically implicated in SMC degeneration and AAA pathogenesis, was also shown to be reduced at mRNA level upon aortic PERK silencing (Fig. S2B). Concomitantly, the mRNA level of macrophage marker CD68 also decreased numerically, in line with the established role of MCP1 as a chemoattractant for macrophage. Effective PERK silencing was also confirmed at mRNA level (Fig. 3D). Taken together, these in vivo loss-of-function data further corroborate a specific role for PERK-targeting strategies in AAA prevention and treatment.

3.4. Development of an AAA-targeting biomimetic NC drug delivery platform

One of the critical roadblocks barring successful translation of existing and new therapeutic strategies is the lack of effective drug delivery systems tailored for AAA treatment. In response to this unmet need, herein we designed a unique biomimetic nanocluster for targeted delivery of PERKi (Fig. 4A). The nanocluster core was formed spontaneously by PERKi-loaded PAMAM-PLGA-COOH unimolecular nanoparticles in an aqueous solution. To confer lesion-targeting capacity to the NC, the surface of the NC was coated with platelet membrane because platelets have been well documented to specifically home to and enrich in aneurysmal lesion sites (Fig. 4A). To confirm the successful coating of platelet membrane on NC, we conjugated platelet membrane vesicles with DiO dye prior to membrane isolation and extrusion. As shown in Fig. 4B, confocal imaging confirmed the colocalization of Cy5 (conjugated to NC) and DiO dyes (labeled to platelet membrane), suggesting successful biointerfacing [30].

PAMAM-PLGA-OH was synthesized *via* ring-opening polymerization. Then, PAMAM-PLGA-OH was reacted with succinic anhydride to yield PAMAM-PLGA-COOH in order to facilitate the cell membrane coating

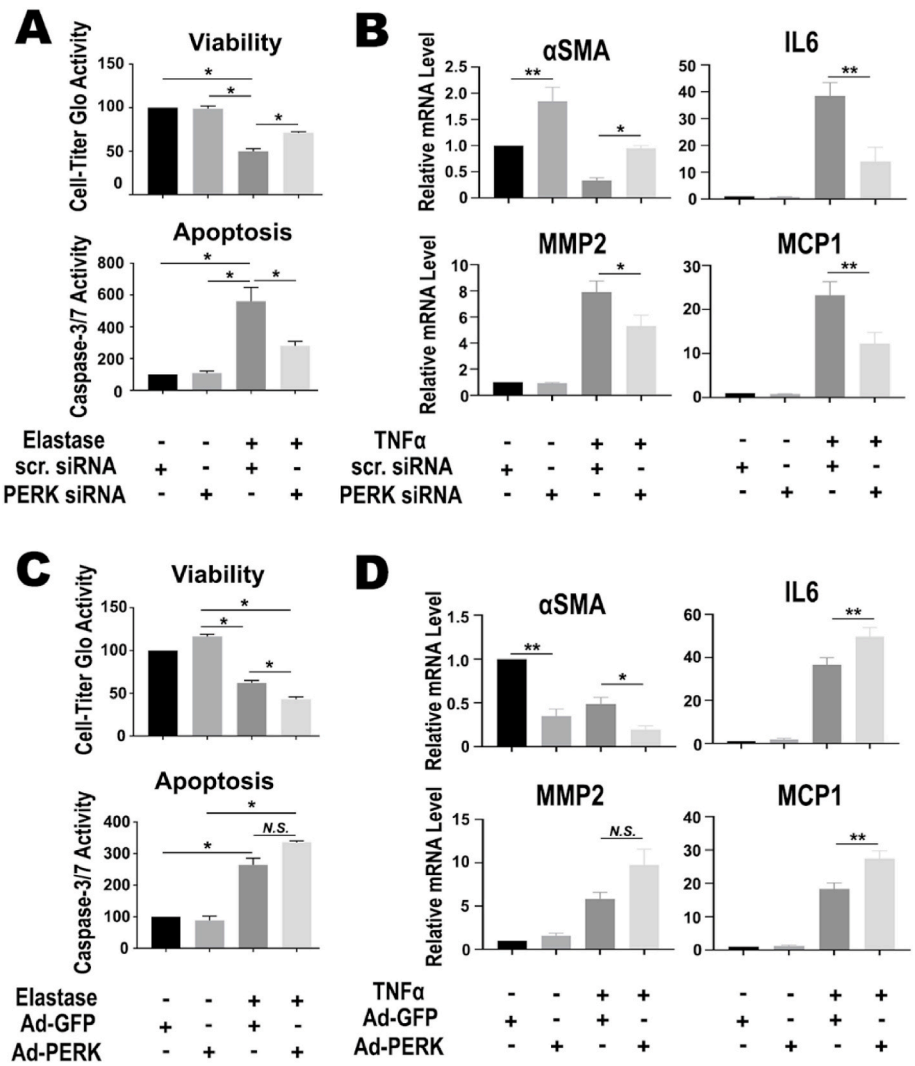

Fig. 2. ***PERK Loss-of-function Reverses, its Gain-of-function Exacerbates SMC Degeneration In Vitro.*** To determine the specific role of PERK in driving the degenerative phenotype transition, human primary aortic SMCs were pretreated with either PERK siRNA (A, B) or overexpressing adenovirus (C, D) to achieve loss- and gain-of-function, respectively. SMCs were then subject to either transient exposure (5 min) to porcine elastase (~1 unit/mL) to stimulate cell death (A, C), or TNFα (10 ng/mL) to induce the dedifferentiated/proteolytic/pro-inflammatory phenotypic transition. A–B: PERK silencing with siRNA. Starved SMCs were transfected with 50 nM PERK-specific siRNA for 48 h and then starved for 24 h prior to elastase or TNFα challenge. (A) Viability of SMCs was determined using CellTiter-Glo assay at 24 h post elastase challenge, and apoptotic index was determined using Caspase-Glo 3/7 assay at 4 h. (B) Quantitation of mRNA levels of inflammatory cytokine (IL6) and macrophage chemoattractant gene (MCP1), ECM proteolytic gene (MMP2), and SMC contractility gene (αSMA) in SMCs with PERK loss-of-function collected at 24 h post TNFα stimulation. (C–D) Adenovirus-mediated PERK gain-of-function. Cells were transduced with PERK-overexpressing adenovirus (Ad-PERK) or GFP control (Ad-GFP) for 6 h, recovered in complete medium for 24 h, followed by starvation for 24 h prior to elastase or TNFα challenge. Similar to A-B, SMC viability and apoptotic index (C), as well as quantitation of mRNA levels of representative genes of the proinflammatory, proteolytic, and SMC contractile genes (D), are presented. Mean ± SEM, n = 4-5; N.S. = no significance, *p < 0.05, **P < 0.01. One-way ANOVA with Tukey post-hoc analysis.

[45]. The initial molecular weight of PAMAM-PLGA-COOH was 90.4 kDa with a polydispersity index (PDI) of 1.39, as measured by GPC (Table S3, Fig. S1D). The degradation profiles of PAMAM-PLGA-COOH were determined by monitoring the weight loss and molecular weight (via GPC) of PAMAM-PLGA-COOH after hydrolysis at pH 5.5 and 7.4 [26,27]. As shown in Fig. S1G, the GPC peak at 23 min (the initial molecular weight of PAMAM-PLGA-COOH) decreased with prolonged storage time for both pH 5.5 (top) and 7.4 (bottom). However, the reduction in the GPC peak at 23 min occurred more rapidly at pH 5.5 than pH 7.4, suggesting faster degradation at acidic condition. This is consistent with the faster weight loss observed at pH 5.5 (Fig. S1F).

In order to track the biomimetic NC in AAA sites and major organs, Cy5-tagged PAMAM-PLGA-COOH was synthesized by conjugating Cy5 onto the surface of PAMAM-PLGA-COOH via an amidation reaction (Fig. 4C). The PERKi loading content in the biomimetic NC quantified by HPLC was 19.8%. The hydrodynamic diameter of the PAMAM-PLGA-COOH unimolecular nanoparticle was 28.8 nm in chloroform. The size of platelet membrane vesicle was 167.2 nm, and its zeta potential was −34.9 mV. The hydrodynamic diameter of the platelet membrane-coated NC was 195.8 nm and its zeta potential was −26.4 mV (Table S3, Fig. S1E). Furthermore, the diameter of the spherical biomimetic NC was round 170 nm under TEM (Fig. 4D, S1E). Furthermore, the biomimetic NC enabled targeted delivery of the hydrophobic PERKi with a biphasic controlled release profile. Fig. 4E shows the release profile of PERKi from the biomimetic NC in PBS (pH 7.4) with 2% tween80 at 37 °C for 45 days. The biomimetic NC exhibited an initial burst release (~57% release within 24 h) to exert prompt control of the highly active degenerative events within the aortic wall. Following the bolus phase, the biomimetic NC continued to provide a sustained release of the remaining PERKi over the course of at least 1 month (~87% release by 27 days) — a feature that is most desirable for the long-term management of the progressively dilating AAA lesions via potentially reducing the overall drug dose required.

To investigate the biomimetic NC's homing ability to AAA lesions, we prepared the biomimetic NC using Cy5-conjugated PAMAM-PLGA-COOH. In an elastase-induced AAA model that features an aggressive disease course that plateaus at day 7 post operation, we injected the biomimetic NC via tail vein at different time points and harvested the whole aortas (from arch to iliac bifurcation) for *ex vivo* IVIS imaging 24 h post injection. As shown in the bright-field images, the abdominal aortic segments progressively dilated in a chronological order, representing the nascent (1 day), small (3 days), and fully established (7 days) AAA lesions (Fig. 5A). In stark contrast to the minimal signals detected in the sham surgery controls, the aneurysmal lesion segments collected at all three stages of AAA development demonstrated strong enrichment of Cy5 fluorescent signals (Fig. 5B). Additionally, the organ distribution of the biomimetic NC is also provided in Fig. 5C and D, showing relatively low non-specific organ retention. Similarly, using a recently established murine AAA model that features a slower yet more chronic disease course, the AAA-lesion targeting capability of the biomimetic NC was

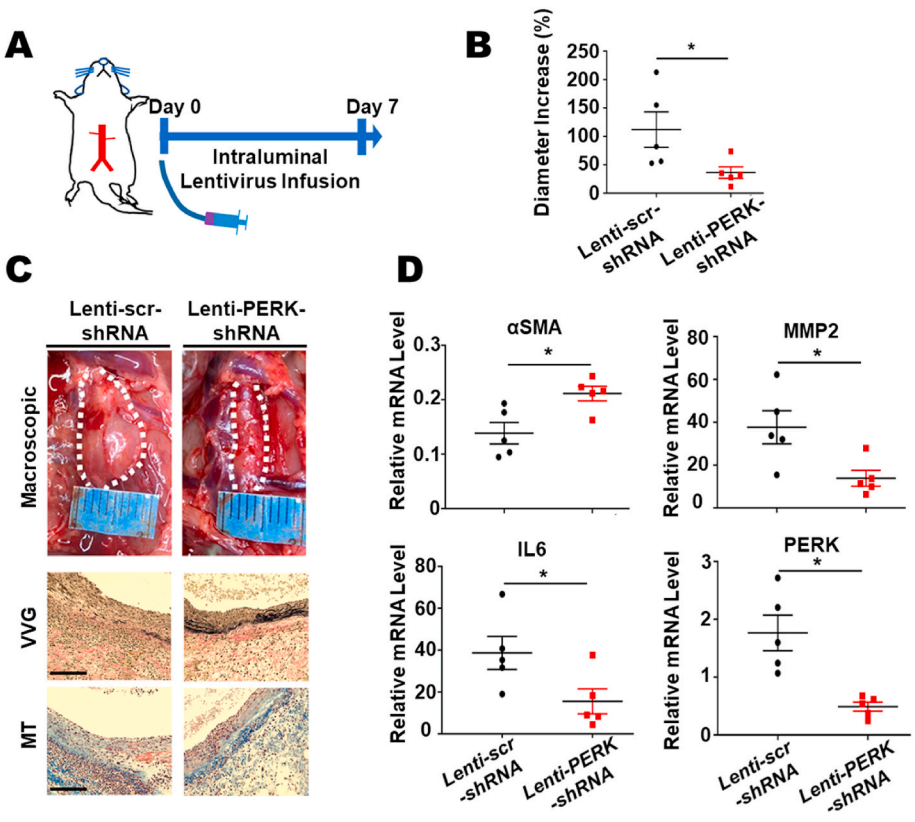

Fig. 3. ***Local PERK Silencing Conferred Effective Control over Development of Elastase-induced AAA Lesions.*** Lentivirus expressing either scrambled control or PERK-specific shRNA was intraluminally infused immediately after the porcine elastase challenge to create AAA lesion. Aorta segments were collected at day 7 post the procedure for analysis. (A) Overview of experimental design. (B) Analysis of aortic diameter increase (fold change of maximal diameters at day 7 versus day 0 baseline). (C) Representative images of AAA lesions at macroscopic and microscopic levels (VVG: elastin staining shown as the black, wavy structure; MT: collagen staining shown in blue, and muscle content shown in red) at day 7 post procedure. Scale bar: 125 μm. (D) Tissue homogenate mRNA analysis of AAA-signature gene expression changes. Quantitation of mRNA levels of inflammatory cytokine genes (IL6), ECM proteolytic genes (MMP2), and SMC contractility gene (αSMA) in AAA segments from elastase-challenged aortic segments. Mean ± SEM, n = 5 rats; *p < 0.05. Mann-Whitney nonparametric test.

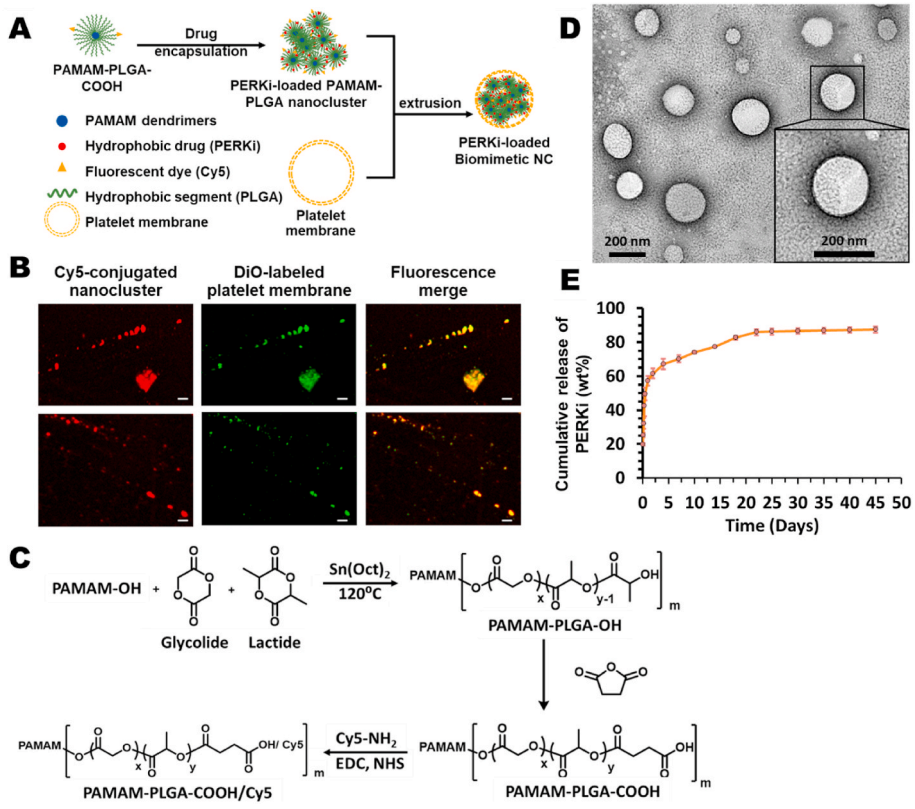

Fig. 4. ***Design and Characterization of an AAA-targeting Biomimetic NC.*** (A) Overview/Illustration of experimental design. Drug-encapsulated biomimetic NC were prepared using extrusion method. (B) Confocal images demonstrating the successful coating process of biomimetic nanocluster. The merged fluorescence images show the colocalization of Cy5 and DiO which were labeled with PAMAM-PLGA-COOH and platelet membrane, respectively. Scale bars: 10 μm. (C) Synthesis schemes of PAMAM-PLGA-OH, PAMAM-PLGA-COOH and PAMAM-PLGA-COOH/Cy5. (D) TEM images of the platelet membrane-coated NC. Scale bars: 200 nm. (E) The *in vitro* release profile of PERKi from biomimetic NC in PBS (pH 7.4) with 2% tween80 at 37 °C. Mean ± SEM, n = 3.

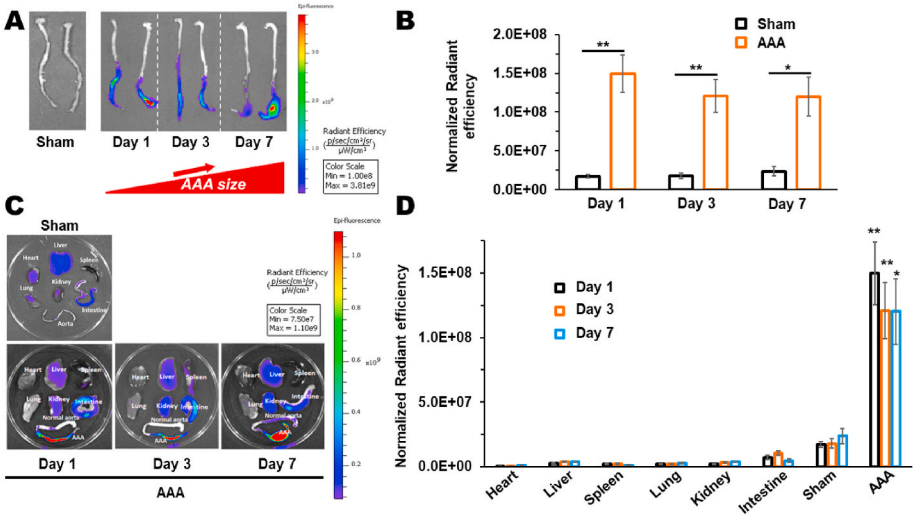

Fig. 5. ***Biodistribution of the biomimetic NC in a rat AAA model.*** Elastase-challenged rats or the sham control (perfused with heat-inactivated elastase) were intravenously injected with Cy5-loaded biomimetic NC. Aortas and other major organs from rats collected at day 1 (nascent AAAs), day 3 (small AAAs), and day 7 (fully established AAAs) were imaged using an IVIS spectrum luminescence system and were compared with those from the sham control. (A) Homing of the biomimetic NC to experimental AAA lesions of different stages. (B) Normalized radiant efficiency of AAA lesions (Fig. 5A) was determined based on Cy5 signal intensities captured (Ex/Em: 650/720 nm) after normalization to tissue weight. (C) Representative IVIS images of the major organs (heart, liver, spleen, lung, kidney, intestine, aorta). (D) Normalized radiant efficiency of major organs (Fig. 5C) was determined based on Cy5 signal intensities captured (Ex/Em: 650/720 nm) after normalization to tissue weight. Data are presented as mean ± SEM with n = 4 or 5 rats per group. Statistical analysis was performed using one-way ANOVA with Tukey's post hoc analysis. *P < 0.05, **P < 0.01 between the respective AAA and sham groups at each time point. Mean ± SEM, n = 4-5 rats; *P < 0.05, **P < 0.01. One-way ANOVA with Tukey post-hoc analysis.

also demonstrated (Fig. S3). To examine the *in situ* localization and cellular uptake of the biomimetic NC in AAA lesion sites, co-immunostainings with antibodies specific to SMC (αSMA) and macrophage markers (CD68) were conducted on frozen sections from the aforementioned aortic specimens. As shown in Fig. S3D, Cy5 fluorescence signal – indicative of NC – were mostly observed in the medial layer, especially SMC; on the other hand, colocalization with $CD68^{+}$ macrophages that predominantly infiltrated into the adventitia was sparse. Overall, these data collectively provided strong evidence supporting the specific AAA-targeting ability of the platelet membrane-coated NC platform, particularly toward the medial SMC.

3.5. Targeted delivery of PERK inhibitor prevents AAA formation

To explore the preventative value of PERK inhibition on AAA development, we applied the AAA lesion-homing NC to achieve targeted delivery of GSK2656157, a second-generation PERK inhibitor (abbreviated as PERKi) [23]. Based on our prior proof-of-concept study and the *in vitro* drug release profile, we provided a single dose regimen (2.5 mg/kg payload) intravenously injected immediately after the elastase-perfusion procedure in rats (Fig. 6A). On day 7, macroscopic analysis revealed a profound beneficial effect of the targetedly delivered PERKi via the biomimetic NC (abbreviated as PERKi-NC) on halting the aneurysmal expansion, with at least 30% reduction in aortic diameter (Fig. 6B) in comparison to either saline injection (abbreviated as Saline),

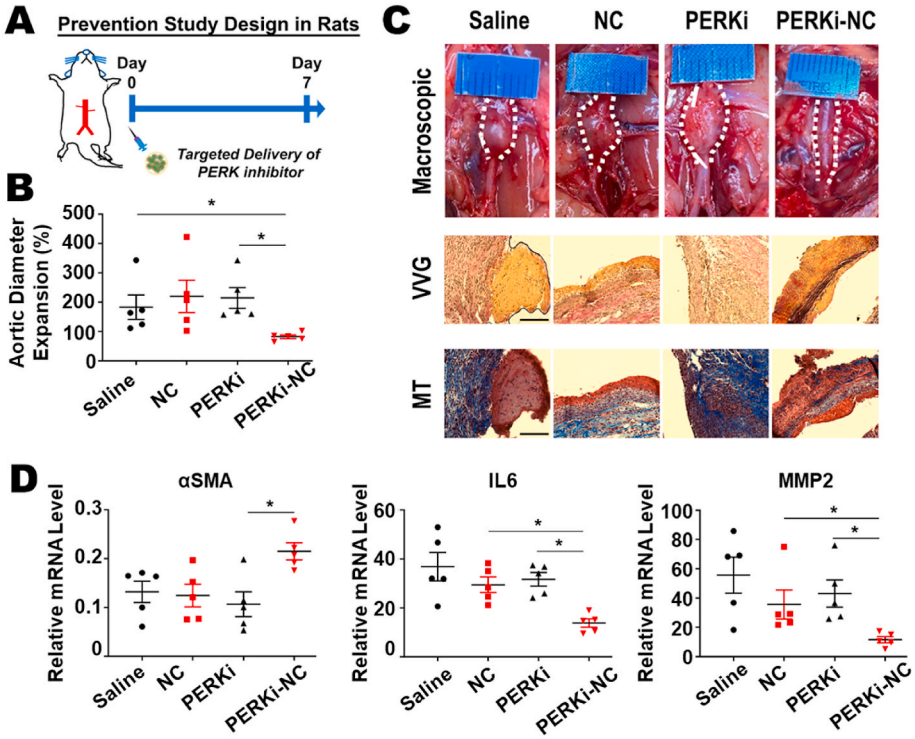

Fig. 6. ***Targeted Delivery of PERK Inhibitor Prevented AAA Formation.*** Targeted delivery of a selective PERK inhibitor prevented the elastase-induced aortic dilation and degeneration in a rat model. (A) Overview of experimental design. Immediately following the elastase-infusion procedure, rats were randomly assigned to a one-time intravenous injection with the following four treatments (all equivalent to 10 mg/kg payload): saline control (Saline), empty NC control (NC), free PERK inhibitor GSK2656157 (PERKi), and GSK2656157-encapsulated biomimetic NC (PERKi-NC). (B) Analysis of aortic diameter increase (fold change of maximal diameters at day 7 versus day 0 baseline). Mean ± SEM, n = 5-6 rats, *p < 0.05. One-way ANOVA with Tukey post-hoc analysis. (C) Representative images of AAA lesions at macroscopic and microscopic levels (VVG: elastin staining shown as the black, wavy structure; MT: collagen staining shown in blue, and muscle content shown in red) at day 7 post procedure. Scale bar: 125 μm. (D) Tissue homogenate mRNA analysis of AAA-signature gene expression changes. Quantitation of mRNA levels of inflammatory cytokine genes (IL6), ECM proteolytic genes (MMP2), and SMC contractility gene (αSMA) in AAA segments from elastase-challenged aortic segments. Mean ± SEM, n = 5 rats, *p < 0.05. One-way ANOVA with Tukey post-hoc analysis.

free form PERKi (abbreviated as PERKi), or empty biomimetic nanoclusters (abbreviated as NC). Histologically, targeted PERK inhibition led to improved vascular remodeling, as evidenced by preserved elastin integrity and collagen content (Fig. 6C). Moreover, mRNA analysis of the lesion tissue homogenates showed significantly reduced expression of aforementioned marker genes of SMC degeneration, IL6 and MMP2. Effective restoration of smooth muscle maturation markers such as αSMA (Fig. 6D) and Myh11 (Fig. S4A) was also documented. Despite a numerical reduction, no statistical difference was observed among the treatment groups regarding macrophage-related markers such as MCP1 and CD68 (Fig. S4C). Additionally, no signs of systemic toxicity were observed based on histological evaluation of key organs (Fig. S5A) as well as qPCR analysis of tissue damage marker expressions in liver and spleen (Fig. S5B). To our knowledge, thus far, our data herein provides the first in vivo evidence supporting the anti-AAA efficacy of PERK-targeting therapy.

3.6. A Weekly Regimen of Targeted PERK inhibition therapy halts the growth of pre-existing AAA lesions

As summarized in a recent meta-analysis, there is a lack of intervention studies to treat pre-existing aneurysmal lesions [46,47]. To better evaluate the interventional potential of our new therapy, we adopted a weekly regimen (2.5 mg/kg payload) starting at day 7 post procedure when established AAAs already formed (Fig. 7A) — a study design that has been widely adopted in existing reports concerning AAA intervention [36,48]. In this particular study, we chose a modified murine model of AAA based on recent reports, which features a chronic yet progressive disease course of aneurysmal dilation [35]. The addition of BAPN, a nonreversible inhibitor for the collagen/elastin-crosslinking enzyme lysyl oxidase (LOX), robustly leads to disruption of the elastic laminae and increases the risk of aneurysmal rupture, recapitulating the natural effects of aging as observed in elderly populations [49,50]. Non-invasive ultrasound imaging confirmed the presence of established AAA lesions (defined as >50% dilation of maximal inner aortic diameter) at day 7 post procedure (Fig. S6). As aforementioned, IVIS study confirmed the capacity of Cy5-conjugated biomimetic NC to specifically home to pre-existing AAAs in this model (Fig. S3). At the 4-week endpoint, extensive aneurysmal dilations could be observed in all three control groups that received either saline (Saline), free solution of PERKi (PERKi), or empty nanocluster injections (NC); in stark contrast, while AAA lesions still persisted in mice that received targeted PERK inhibition therapy (PERKi-NC), the progression of the pre-existing aneurysms was significantly hampered (Fig. 7C and Fig. S6C). Improved histological features (e.g., elastin and collagen structures) were associated with the treatment of targeted PERKi (Fig. 7B). Similarly,

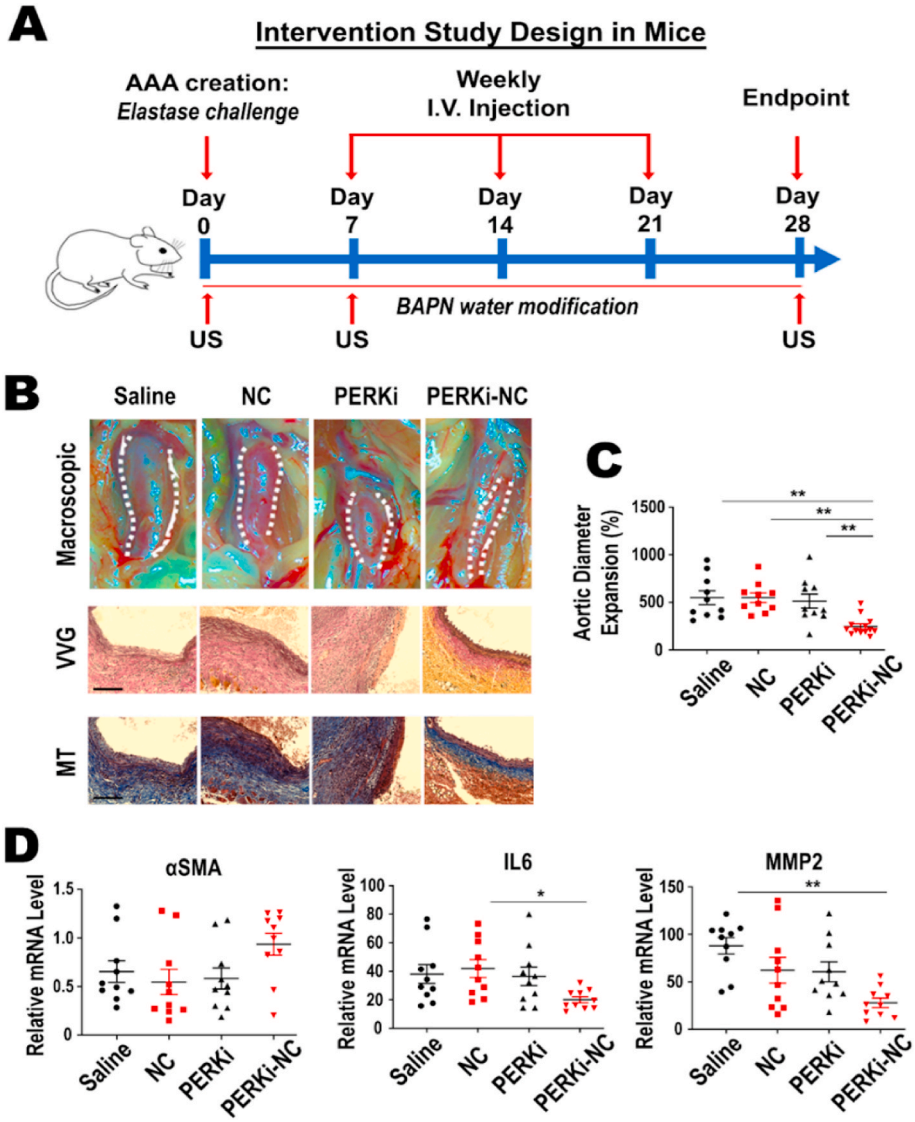

Fig. 7. *A Weekly Regimen of Targeted PERK Inhibition Therapy Halted the Growth of Pre-existing AAA lesions.* (A) Overview of experimental design. A modified murine model was used to recapitulate the chronic disease progression of AAA. Ultrasound (abbreviated as US) imaging was performed at indicated time points as described in Supplementary Document. At day 7 post topical elastase application, mice with establish AAA lesions were randomly assigned to a weekly regimen with the following four treatments (all equivalent to 10 mg/kg payload): saline control (Saline), empty NC control (NC), free PERK inhibitor GSK2656157 (PERKi), and GSK2656157-encapsulated biomimetic NC (PERKi-NC). (B) Representative images of AAA lesions at macroscopic and microscopic levels (VVG: elastin staining shown as the black, wavy structure; MT: collagen staining shown in blue, and muscle content shown in red) at day 28 post procedure. Scale bar: 125 μm. (C) Analysis of aortic diameter increase (fold change of maximal diameters at day 28 versus day 0 baseline). Mean ± SEM, n = 10-12 mice. **P < 0.01. One-way ANOVA with Tukey post-hoc analysis. (D) Tissue homogenate mRNA analysis of AAA-signature gene expression changes. Quantitation of mRNA levels of inflammatory cytokine genes (IL6), ECM proteolytic genes (MMP2), and SMC contractility gene (αSMA) in AAA segments from elastase-challenged aortic segments. Mean ± SEM, n = 10 mice. *P < 0.05, **P < 0.01. One-way ANOVA with Tukey post-hoc analysis.

characteristics of SMC degeneration, including increased pro-inflammatory/proteolytic (IL6/MMP2) and reduction in maturation/differentiation gene expression (αSMA/Myh11), were robustly mitigated upon the targeted delivery of PERKi (Fig. 7D and S7A). Reduction in MCP1 and CD68 levels — indicative of decreased macrophage infiltration — was also documented upon targeted PERKi (Fig. S7C). Consistent with the significantly reduced overall drug dose, the overall safety profile of the current weekly regimen was confirmed with the lack of systemic toxicities (Fig. S8).

4. Discussion

Abdominal aortic aneurysm (AAA) is a common disease in aged populations, diagnosed as at least 1.5-fold focal dilation of the abdominal aorta [1]. Surgical repair, even though risky and expensive, is the only treatment available for AAA [4]. Thanks to improved non-invasive screening technologies, an increasing number of AAAs are being detected [51,52]. However, the majority of these are characterized as small AAA (<5.5 cm in men; <5 cm in women) not elected for surgical repair [53,54]. Current clinical evidence suggests that AAA size alone does not provide a fully reliable prediction of aneurysmal rupture as a single parameter, and patients with small yet greater than 3.5 cm AAAs are still at risk [54]. Ruptured small AAA has been reported to constitute around 10%–17% of all ruptured AAA cases [55–57]. Therefore, there is a compelling medical need to discover safe (non-surgical) drug therapy to stabilize small AAA lesions from progressing to deadly rupture [7]. As populations age rapidly, this need is mounting and imminent [58].

The search for effective drug treatment of AAA has been actively ongoing for decades. Extensive clinical trials have been conducted with anti-hypertensive (e.g., propranolol and perindopril) [59,60] and lipid-lowering medications (fenofibrate) [61], proteolytic inhibitors (e.g., doxycycline) [4,5,19], and other miscellaneous classes of drugs (e.g., anti-platelet therapy) [62], albeit none has demonstrated definitive clinical benefits. Two FDA-approved drugs, rapamycin and metformin, emerge as promising candidates to be repurposed for treatment of small diameter AAAs, although definitive clinical efficacies are yet to be seen [33,63–65]. In recent years, numerous molecular mechanisms and targets have been discovered to be critically implicated in the degeneration of SMC and hence AAA pathogenesis, e.g., programmed cell death pathways [44], non-coding RNAs [66–68], SMC de-differentiation transcription factors [15,69,70] etc. However, the majority of these molecular targets are either "undruggable" or associated with significant "off-target" complications of existing drugs, thereby severely compromising translational perspectives. In this regard, further exploration of new disease drivers of AAA, particularly those with available selective agonists/antagonists, are certainly warranted.

The current study provides the very first proof-of-concept evidence to support PERK as viable intervention target for AAA. Previously, our group established PERK as a key driver in promoting the hyperplastic and de-differentiated phenotype transition of SMCs [31,32]. Although the excessive activation of PERK and other ER stress response proteins has been documented in prior studies surveying experimental and clinical AAAs, there is no literature documenting the specific role of PERK in SMC degeneration and aneurysmal diseases [38]. Using both gain- and loss-of-function approaches *in vitro*, we demonstrated a clear role of PERK in dictating all salient phenotypes of SMC degeneration, including cell death, inflammation (e.g., induction of cytokine and chemoattractant gene expressions), proteolysis, and de-differentiation. Our observation of PERK's role as a "master regulator" of SMC phenotype transition is line with recent reports in the context of vascular calcification and atherosclerosis [71–74]. Moreover, our in vivo studies further indicated that tuning down PERK through either genetic silencing or targeted delivery of selective PERKi effectively prevent AAA lesion formation in an elastase-induced model in rats. Additionally, excessive activation of PERK was also noted in lesion-infiltrating macrophages, which constitute another key cellular population that critically contributes to AAA pathogenesis. Indeed, PERK has been widely shown to be a molecular driver of macrophage activation, including recent reports in cardiovascular disease models [75]. It is worth noting that our in vivo loss-of-function approaches primarily target the medial layer, primarily occupied by SMC. Nevertheless, a macrophage-specific role of ER stress PERK pathway in AAA pathogenesis cannot be excluded, which warrants future investigations. In fact, non-discriminately blocking PERK in multiple disease-driving cell types (e.g., SMC and macrophages) specifically in AAA lesion sites may offer more effective therapeutic efficacy.

Together with our prior reports of the endothelium-protective and anti-thrombotic benefits of PERK blockade therapy [31,32] — both of which are highly desirable in the management of aneurysmal diseases [22], we contend that PERK confer a novel opportune target for treatment of AAA.

Recent years witnessed a growing interest in the implication of ER stress in aneurysmal diseases [38,39]. In fact, the therapeutic effects of pan-ER stress pacification with promiscuous inhibitors (e.g., tauroursodeoxycholic acid, intermedin1-53) have previously been documented in multiple recent reports [76,77]. Global deletion of CHOP, a common downstream effector shared by all three ER stress response pathways, led to reduced aneurysm formation and dissection, further highlighting the significance of aberrant ER stress reponses in aneurysmal diseases [40,41]. However, most preceding studies failed to dissect the specific role of each individual branch within the ER stress response, namely the PERK pathway, IRE1/XBP1 pathway, and ATF6 pathway. Data derived from other disease categories informed the functional non-redundancy and distinct biological outcomes of targeting the three pathways [78]. To date, there is only one existing report on the detailed mechanistic contribution of individual ER stress pathways in aneurysm [79]. In this study, the authors probed the role of IRE1/XBP1 pathway in regulating SMC phenotype maintenance, and deleting unspliced XBP1, the substrate of the IRE1 kinase, exacerbated aortic aneurysm lesion in a SMC-specific knockout model. Given the paucity of in-depth studies on this topic, it is of both mechanistic and therapeutic interests to specifically probe the PERK branch of ER stress response in the context of SMC degeneration and AAA.

Despite the rising interest in new drug/target development and repurposing efforts, none have yielded an FDA-approved drug therapy for AAA. This bleak reality presses an urgent need for a paradigm shift to more sophisticated precision drug delivery. Indeed, in the absence of a targeted delivery formulation, prior clinical trials of promising AAA therapeutics (e.g., doxycycline) and ER stress inhibitors (e.g., PERKi) have been universally plagued with issues such as poor pharmacokinetic and pharmacodynamic properties or systemic toxicity, which significantly limit their therapeutic development and translation [4,7,80]. Judiciously designed nanotechnologies have been widely developed for imaging and targeted delivery in cardiovascular diseases, representing a promising avenue to help achieve the optimal therapeutic outcomes of PERKi [81].

However, as summarized in our recent review, research efforts on AAA-targeting nanotechnologies are surprisingly limited [22]. Over the last few years, we and others have developed a series of biomimetic nanoplatforms via biointerfacing with rationally chosen cell membrane coatings [82–86]. Such biomimicry concept has been widely adopted for a spectrum of disease applications; as for aneurysmal diseases, the only existing report described a macrophage-mimetic nanoparticle with surface conjugation of αvβ3 integrin-targeting peptide cRGD, which enabled targeted delivery of rapamycin to aneurysmal lesions in a calcium chloride-induced model in rats [87]. Since platelet aggregation and accumulation are highly prevalent features in AAAs, we hypothesized that a platelet-inspired design with platelet membrane coating could enable aneurysm-homing capacity. Indeed, our rationally designed platelet-mimetic nanoclusters displayed highly specific enrichment at both nascent and full-sized AAA lesions in elastase-induced rodent models, and were taken up predominantly by

SMC in the medial layers of aneurysmal aortas. As shown in other cardiovascular disease models, such lesion targeting capacity is likely mediated by the panel of adhesion molecules present on the outer surface of the platelet membrane, including integrins and transmembrane glycoproteins that could specifically bind to the exposed extracellular matrix proteins (e.g., collagen IV) in the aneurysmal aortas [82]. Additionally, this innovative delivery platform enabled targeted delivery of the hydrophobic PERKi with a biphasic controlled release profile. The PAMAM-PLGA nanocluster core was designed to achieve an initial burst release (~60% release within 24 h) to exert prompt control of the highly active degenerative events within the aortic wall. Following the bolus phase, the nanoclusters could continue to provide a sustained release of the remaining PERKi over the course of at least 1 month (~85% release by 27 days) — a feature that is most desirable for the long-term management of the progressively dilating AAA lesions. Sustained drug release enabled by biomimetic nanoclusters can ultimately lead to effective control of experimental AAA lesions at a dramatically reduced overall drug dosage (a 2.5 mg/kg, weekly regimen versus the conventional 50 mg/kg, twice to three times daily regimens for existing PERK inhibitors) [23,80]. This presents a significant improvement, as severe systemic toxicities have been documented with existing ER stress inhibitors delivered through traditional routes [80]. We contend that other investigative AAA therapeutics plagued with suboptimal in vivo drug performances could broadly benefit from this drug delivery platform for future improvement.

Another major accomplishment of our current study lies in the interventional potential of our targeted PERK inhibition therapy in halting the progression of pre-existing AAAs. Indeed, patients typically already bear existing AAA lesions at the time of diagnosis. It thus remains an imperative task to translate research into effective intervention for existing AAA. At the moment, how to stabilize an already formed AAA lesion still remains the top challenge in both basic and clinical arenas [47]. Unfortunately, a bleak reality is that the vast majority of past pre-clinical studies rather adopted a preventative study design — that is, the experimental treatments were administered either prior to or at the time of AAA induction procedures, when the experimental aneurysms were not yet formed. In a recent meta-analysis, merely 35 out of 4758 published works were identified as intervention studies [46]. Our current study adds to this short list of research endeavors aimed at the ultimate translation into clinical utility for the intervention of pre-existing AAAs.

A major limitation of this proof-of-concept study is the use of only one experimental inducer of AAA in rodents. In our current study, local application of porcine pancreatic elastase was used to induce the initial destruction of elastic integrity, followed by subsequent loss of SMC, immune cell infiltration, and ECM destruction. This methodology has been widely used to study the acute onset phase (short-term) as well as the long-term progression (long-term, with the incorporation of BAPN), which is ideal to determine both the preventive and interventional efficacy of the biomimetic NC-based PERKi therapy. The advent of recent single-cell RNA sequencing (scRNA-seq) efforts, especially the comparative analysis of clinical and elastase-induced experimental AAA specimens, further supports the notion that the elastase model is well suited to study the role of SMC degeneration and other pathological components (e.g., macrophage infiltration) in the onset and progression of AAA [88,89]. Nevertheless, we acknowledge the limitations that we may not be able to extrapolate the role of PERK based on results derived from only one experimental model. Indeed, as summarized in our recent reports and others, no single experimental model could fully recapitulate the pathophysiological features of clinical AAA. Other commonly used models, including the angiotensin II (AngII) model and the calcium model, each has their unique advantages in terms of clinical relevance, such as the involvement of hypertension, hypercholesterolemia, and aortic calcification. To further strengthen the mechanistic significance and potential clinical utility, future studies in additional mouse models of AAA are warranted.

5. Conclusions

Despite the prevalence and lethality of AAAs, there are still no drug therapies nor tailored drug delivery platforms with proven clinical benefits. Our study provides the first evidence that the ER stress PERK kinase critically contributes to the degenerative phenotypic transitions of SMCs and hence presents a viable intervention target for AAA management. Moreover, we developed a biomimetic nanocluster platform that enables targeted delivery of selective PERK inhibitors to AAA lesions in experimental models. Such targeted PERK inhibition therapy not only demonstrates clear preventative benefits against AAA formation, and when administered to animals with pre-existing AAAs, it also demonstrates clear interventional benefits in stopping the chronic progression of aneurysmal dilation — a key feature that was often missing in the majority of prior research efforts concerning AAA therapies.

Protocol statement

All animal studies conform to the National Institutes of Health Guide for the Care and Use of Laboratory Animals. Research protocols are approved by the Institutional Animal Care and Use Committees and Institutional Biosafety Committee at University of Virginia. Human specimens were obtained under approved institutional review board (IRB).

CRediT authorship contribution statement

Nisakorn Yodsanit: Investigation, Methodology, Writing – original draft. **Takuro Shirasu:** Investigation, Methodology, Writing – original draft. **Yitao Huang:** Investigation, Methodology. **Li Yin:** Investigation, Methodology. **Zain Husain Islam:** Investigation, Methodology. **Alexander Christopher Gregg:** Investigation, Methodology. **Alessandra Marie Riccio:** Investigation, Methodology. **Runze Tang:** Investigation, Methodology. **Eric William Kent:** Investigation, Methodology. **Yuyuan Wang:** Investigation. **Ruosen Xie:** Conceptualization, Investigation. **Yi Zhao:** Conceptualization, Investigation. **Mingzhou Ye:** Investigation. **Jingcheng Zhu:** Investigation. **Yi Huang:** Investigation, Methodology. **Nicholas Hoyt:** Investigation, Methodology. **Mengxue Zhang:** Investigation, Methodology. **John A. Hossack:** Investigation, Methodology. **Morgan Salmon:** Investigation, Methodology. **K. Craig Kent:** Supervision. **Lian-Wang Guo:** Writing – review & editing, Supervision. **Shaoqin Gong:** Writing – review & editing, Supervision. **Bowen Wang:** Writing – original draft, Writing – review & editing, Supervision.

Declaration of competing interest

The authors declare that they have no known competing financial interests or personal relationships that could have appeared to influence the work reported in this paper.

Acknowledgements

This work was supported by the National Institute of Health (NIH) grants R01HL133665 (to L.-W.G.), R01HL143469, R01HL129785 (to K. C.K, S.G., and L.-W.G.), R01HL162895 (to B.W.), R01HL132395 and 1S10RR027333 (to J.A.H.), and Overseas Research Fellowships, The Uehara Memorial Foundation in Japan (to T.S.). We thank Dr. Xinyu Zhou for the technical instruction and support with Confocal microscopy.

Appendix A. Supplementary data

Supplementary data to this article can be found online at https://doi.org/10.1016/j.bioactmat.2023.02.009.

References

[1] N. Sakalihasan, R. Limet, O.D. Defawe, Abdominal aortic aneurysm, Lancet 365 (9470) (Apr 30-May 6 2005) 1577–1589, https://doi.org/10.1016/S0140-6736(05)66459-8.

[2] N.L. Weintraub, Understanding abdominal aortic aneurysm, N. Engl. J. Med. 361 (11) (Sep 10 2009) 1114–1116, https://doi.org/10.1056/NEJMcibr0905244.

[3] F.A. Lederle, R.L. Kane, R. MacDonald, T.J. Wilt, Systematic review: repair of unruptured abdominal aortic aneurysm, Ann. Intern. Med. 146 (10) (May 15 2007) 735–741, https://doi.org/10.7326/0003-4819-146-10-200705150-00007.

[4] B.T. Baxter, J. Matsumura, J. Curci, et al., Non-invasive Treatment of Abdominal Aortic Aneurysm Clinical Trial (N-TA(3)CT): design of a Phase IIb, placebo-controlled, double-blind, randomized clinical trial of doxycycline for the reduction of growth of small abdominal aortic aneurysm, Contemp. Clin. Trials 48 (May 2016) 91–98, https://doi.org/10.1016/j.cct.2016.03.008.

[5] B.T. Baxter, J. Matsumura, J.A. Curci, et al., Effect of doxycycline on aneurysm growth among patients with small infrarenal abdominal aortic aneurysms: a randomized clinical trial, JAMA 323 (20) (May 26 2020) 2029–2038, https://doi.org/10.1001/jama.2020.5230.

[6] A.M. Knops, A. Goossens, D.T. Ubbink, et al., A decision aid regarding treatment options for patients with an asymptomatic abdominal aortic aneurysm: a randomised clinical trial, Eur. J. Vasc. Endovasc. Surg. 48 (3) (Sep 2014) 276–283, https://doi.org/10.1016/j.ejvs.2014.04.016.

[7] K. Kurosawa, J.S. Matsumura, D. Yamanouchi, Current status of medical treatment for abdominal aortic aneurysm, Circ. J. 77 (12) (2013) 2860–2866, https://doi.org/10.1253/circj.cj-13-1252.

[8] T. Shirasu, H. Takagi, J. Yasuhara, T. Kuno, K.C. Kent, W.D. Clouse, Smaller size is more suitable for pharmacotherapy among undersized abdominal aortic aneurysm: a systematic review and meta-analysis, Vasc. Med. (Dec 20 2021), https://doi.org/10.1177/1358863X211061603, 1358863X211061603.

[9] I. Hinterseher, G. Tromp, H. Kuivaniemi, Genes and abdominal aortic aneurysm, Ann. Vasc. Surg. 25 (3) (Apr 2011) 388–412, https://doi.org/10.1016/j.avsg.2010.09.004.

[10] R.A. Quintana, W.R. Taylor, Cellular mechanisms of aortic aneurysm formation, Circ. Res. 124 (4) (Feb 15 2019) 607–618, https://doi.org/10.1161/CIRCRESAHA.118.313187.

[11] Z. Cheng, Y.Z. Zhou, Y. Wu, et al., Diverse roles of macrophage polarization in aortic aneurysm: destruction and repair, J. Transl. Med. 16 (1) (Dec 13 2018) 354, https://doi.org/10.1186/s12967-018-1731-0.

[12] J. Raffort, F. Lareyre, M. Clement, R. Hassen-Khodja, G. Chinetti, Z. Mallat, Monocytes and macrophages in abdominal aortic aneurysm, Nat. Rev. Cardiol. 14 (8) (Aug 2017) 457–471, https://doi.org/10.1038/nrcardio.2017.52.

[13] N. Airhart, B.H. Brownstein, J.P. Cobb, et al., Smooth muscle cells from abdominal aortic aneurysms are unique and can independently and synergistically degrade insoluble elastin, J. Vasc. Surg. 60 (4) (Oct 2014) 1033–1041, https://doi.org/10.1016/j.jvs.2013.07.097. ; discussion 1041-2.

[14] G. Li, M. Wang, A.W. Caulk, et al., Chronic mTOR activation induces a degradative smooth muscle cell phenotype, J. Clin. Invest. 130 (3) (Mar 2 2020) 1233–1251, https://doi.org/10.1172/JCI131048.

[15] M. Salmon, W.F. Johnston, A. Woo, et al., KLF4 regulates abdominal aortic aneurysm morphology and deletion attenuates aneurysm formation, Circulation 128 (11 Suppl 1) (Sep 10 2013) S163–S174, https://doi.org/10.1161/CIRCULATIONAHA.112.000238.

[16] Z. Chang, G. Zhao, Y. Zhao, et al., BAF60a deficiency in vascular smooth muscle cells prevents abdominal aortic aneurysm by reducing inflammation and extracellular matrix degradation, Arterioscler. Thromb. Vasc. Biol. 40 (10) (Oct 2020) 2494–2507, https://doi.org/10.1161/ATVBAHA.120.314955.

[17] M. Imanishi, S. Tomita, K. Ishizawa, et al., Smooth muscle cell-specific Hif-1alpha deficiency suppresses angiotensin II-induced vascular remodelling in mice, Cardiovasc. Res. 102 (3) (Jun 1 2014) 460–468, https://doi.org/10.1093/cvr/cvu061.

[18] T. Hadi, L. Boytard, M. Silvestro, et al., Macrophage-derived netrin-1 promotes abdominal aortic aneurysm formation by activating MMP3 in vascular smooth muscle cells, Nat. Commun. 9 (1) (Nov 27 2018) 5022, https://doi.org/10.1038/s41467-018-07495-1.

[19] C.A. Meijer, T. Stijnen, M.N. Wasser, et al., Doxycycline for stabilization of abdominal aortic aneurysms: a randomized trial, Ann. Intern. Med. 159 (12) (Dec 17 2013) 815–823, https://doi.org/10.7326/0003-4819-159-12-201312170-00007.

[20] C.Y. Zhao, R. Cheng, Z. Yang, Z.M. Tian, Nanotechnology for cancer therapy based on chemotherapy, Molecules 23 (4) (Apr 4 2018), https://doi.org/10.3390/molecules23040826.

[21] A. Khurana, P. Allawadhi, I. Khurana, et al., Role of nanotechnology behind the success of mRNA vaccines for COVID-19, Nano Today 38 (Jun 2021), 101142, https://doi.org/10.1016/j.nantod.2021.101142.

[22] N. Yodsanit, B. Wang, Y. Zhao, L.W. Guo, K.C. Kent, S. Gong, Recent progress on nanoparticles for targeted aneurysm treatment and imaging, Biomaterials 265 (Jan 2021), 120406, https://doi.org/10.1016/j.biomaterials.2020.120406.

[23] J.M. Axten, S.P. Romeril, A. Shu, et al., Discovery of GSK2656157: an optimized PERK inhibitor selected for preclinical development, ACS Med. Chem. Lett. 4 (10) (Oct 10 2013) 964–968, https://doi.org/10.1021/ml400228e.

[24] G. Chen, X. Shi, B. Wang, et al., Unimolecular micelle-based hybrid system for perivascular drug delivery produces long-term efficacy for neointima attenuation in rats, Biomacromolecules 18 (7) (Jul 10 2017) 2205–2213, https://doi.org/10.1021/acs.biomac.7b00617.

[25] S. Sam, L. Touahir, J. Salvador Andresa, et al., Semiquantitative study of the EDC/NHS activation of acid terminal groups at modified porous silicon surfaces, Langmuir 26 (2) (Jan 19 2010) 809–814, https://doi.org/10.1021/la902220a.

[26] A. Shibata, S. Yada, M. Terakawa, Biodegradability of poly(lactic-co-glycolic acid) after femtosecond laser irradiation, Sci. Rep. 6 (1) (2016/06/15 2016), 27884, https://doi.org/10.1038/srep27884.

[27] X.S. Wu, N. Wang, Synthesis, characterization, biodegradation, and drug delivery application of biodegradable lactic/glycolic acid polymers. Part II: biodegradation, J. Biomater. Sci. Polym. Ed. 12 (1) (2001/01/01 2001) 21–34, https://doi.org/10.1163/156856201744425.

[28] P. Vangeyte, S. Gautier, R. Jerome, About the methods of preparation of poly(ethylene oxide)-b-poly(epsilon-caprolactone) nanoparticles in water analysis by dynamic light scattering, Colloid. Surface. 242 (1–3) (Aug 2 2004) 203–211.

[29] Z.L. Tyrrell, Y.Q. Shen, M. Radosz, Fabrication of micellar nanoparticles for drug delivery through the self-assembly of block copolymers, Prog. Polym. Sci. 35 (9) (Sep 2010) 1128–1143.

[30] H. He, C. Guo, J. Wang, et al., Leutusome: a biomimetic nanoplatform integrating plasma membrane components of leukocytes and tumor cells for remarkably enhanced solid tumor homing, Nano Lett. 18 (10) (2018/10/10 2018) 6164–6174, https://doi.org/10.1021/acs.nanolett.8b01892.

[31] B. Wang, M. Zhang, G. Urabe, T. Shirasu, L.W. Guo, K.C. Kent, PERK inhibition promotes post-angioplasty Re-endothelialization via modulating SMC phenotype changes, J. Surg. Res. 257 (Aug 29 2020) 294–305, https://doi.org/10.1016/j.jss.2020.05.070.

[32] B. Wang, M. Zhang, G. Urabe, et al., PERK inhibition mitigates restenosis and thrombosis: a potential low-thrombogenic antirestenotic paradigm, JACC Basic Transl Sci 5 (3) (Mar 2020) 245–263, https://doi.org/10.1016/j.jacbts.2019.12.005.

[33] T. Shirasu, H. Koyama, Y. Miura, K. Hoshina, K. Kataoka, T. Watanabe, Nanoparticles effectively target rapamycin delivery to sites of experimental aortic aneurysm in rats, PLoS One 11 (6) (2016), e0157813, https://doi.org/10.1371/journal.pone.0157813.

[34] J. Xiong, S.M. Wang, L.H. Chen, Y. Lin, Y.F. Zhu, C.S. Ye, Elastic fibers reconstructed using adenovirus-mediated expression of tropoelastin and tested in the elastase model of abdominal aortic aneurysm in rats, J. Vasc. Surg. 48 (4) (Oct 2008) 965–973, https://doi.org/10.1016/j.jvs.2008.04.016.

[35] G. Lu, G. Su, J.P. Davis, et al., A novel chronic advanced stage abdominal aortic aneurysm murine model, J. Vasc. Surg. 66 (1) (Jul 2017) 232–242, https://doi.org/10.1016/j.jvs.2016.07.105.

[36] C. Zhang, A. Mohan, H. Shi, C. Yan, Sildenafil (Viagra) aggravates the development of experimental abdominal aortic aneurysm, J. Am. Heart Assoc. 11 (2) (Jan 18 2022), e023053, https://doi.org/10.1161/JAHA.121.023053.

[37] J. Li, G. Urabe, Y. Huang, et al., A role for polo-like kinase 4 in vascular fibroblast cell-type transition, JACC Basic Transl Sci 6 (3) (Mar 2021) 257–283, https://doi.org/10.1016/j.jacbts.2020.12.015.

[38] M. Miyao, S. Cicalese, H.A. Cooper, S. Eguchi, Endoplasmic reticulum stress and mitochondrial biogenesis are potential therapeutic targets for abdominal aortic aneurysm, Clin. Sci. (Lond.) 133 (19) (Oct 15 2019) 2023–2028, https://doi.org/10.1042/CS20190648.

[39] Y. Li, G. Lu, D. Sun, H. Zuo, D.W. Wang, J. Yan, Inhibition of endoplasmic reticulum stress signaling pathway: a new mechanism of statins to suppress the development of abdominal aortic aneurysm, PLoS One 12 (4) (2017), e0174821, https://doi.org/10.1371/journal.pone.0174821.

[40] L.X. Jia, W.M. Zhang, T.T. Li, et al., ER stress dependent microparticles derived from smooth muscle cells promote endothelial dysfunction during thoracic aortic aneurysm and dissection, Clin. Sci. (Lond.) 131 (12) (Jun 1 2017) 1287–1299, https://doi.org/10.1042/CS20170252.

[41] L.X. Jia, W.M. Zhang, H.J. Zhang, et al., Mechanical stretch-induced endoplasmic reticulum stress, apoptosis and inflammation contribute to thoracic aortic aneurysm and dissection, J. Pathol. 236 (3) (Jul 2015) 373–383, https://doi.org/10.1002/path.4534.

[42] G. Ailawadi, C.W. Moehle, H. Pei, et al., Smooth muscle phenotypic modulation is an early event in aortic aneurysms, J. Thorac. Cardiovasc. Surg. 138 (6) (Dec 2009) 1392–1399, https://doi.org/10.1016/j.jtcvs.2009.07.075.

[43] M. Salmon, M. Spinosa, Z.E. Zehner, G.R. Upchurch, G. Ailawadi, Klf4, Klf2, and Zfp148 activate autophagy-related genes in smooth muscle cells during aortic aneurysm formation, Phys. Rep. 7 (8) (Apr 2019), e14058, https://doi.org/10.14814/phy2.14058.

[44] Q. Wang, Z. Liu, J. Ren, S. Morgan, C. Assa, B. Liu, Receptor-interacting protein kinase 3 contributes to abdominal aortic aneurysms via smooth muscle cell necrosis and inflammation, Circ. Res. 116 (4) (Feb 13 2015) 600–611, https://doi.org/10.1161/CIRCRESAHA.116.304899.

[45] R.H. Fang, A.V. Kroll, W.W. Gao, L.F. Zhang, Cell membrane coating nanotechnology, Adv. Mater. 30 (23) (Jun 6 2018).

[46] J. Phie, S. Thanigaimani, J. Golledge, Systematic review and meta-analysis of interventions to slow progression of abdominal aortic aneurysm in mouse models, Arterioscler. Thromb. Vasc. Biol. 41 (4) (Apr 2021) 1504–1517, https://doi.org/10.1161/ATVBAHA.121.315942.

[47] H.S. Lu, A.P. Owens 3rd, B. Liu, A. Daugherty, Illuminating the importance of studying interventions on the propagation phase of experimental mouse abdominal aortic aneurysms, Arterioscler. Thromb. Vasc. Biol. 41 (4) (Apr 2021) 1518–1520, https://doi.org/10.1161/ATVBAHA.121.316070.

[48] B. Xu, Y. Iida, K.J. Glover, et al., Inhibition of VEGF (vascular endothelial growth factor)-A or its receptor activity suppresses experimental aneurysm progression in the aortic elastase infusion model, Arterioscler. Thromb. Vasc. Biol. 39 (8) (Aug 2019) 1652–1666, https://doi.org/10.1161/ATVBAHA.119.312497.

[49] D.J. Romary, A.G. Berman, C.J. Goergen, High-frequency murine ultrasound provides enhanced metrics of BAPN-induced AAA growth, Am. J. Physiol. Heart Circ. Physiol. 317 (5) (Nov 1 2019) H981–H990, https://doi.org/10.1152/ajpheart.00300.2019.
[50] E.W. Remus, R.E. O'Donnell Jr., K. Rafferty, et al., The role of lysyl oxidase family members in the stabilization of abdominal aortic aneurysms, Am. J. Physiol. Heart Circ. Physiol. 303 (8) (Oct 15 2012) H1067–H1075, https://doi.org/10.1152/ajpheart.00217.2012.
[51] E.J. Zucker, A.M. Prabhakar, Abdominal aortic aneurysm screening: concepts and controversies, Cardiovasc. Diagn. Ther. 8 (Suppl 1) (Apr 2018) S108–S117, https://doi.org/10.21037/cdt.2017.09.13.
[52] T.F.X. O'Donnell, B.E. Landon, M.L. Schermerhorn, AAA screening should Be expanded, Circulation 140 (11) (Sep 10 2019) 889–890, https://doi.org/10.1161/CIRCULATIONAHA.119.041116.
[53] J. Brodersen, A. Hansson, M. Johansson, V. Siersma, M. Langenskiold, M. Pettersson, Consequences of screening in abdominal aortic aneurysm: development and dimensionality of a questionnaire, J Patient Rep Outcomes 2 (2017) 37, https://doi.org/10.1186/s41687-018-0066-1.
[54] N. Kontopodis, D. Pantidis, A. Dedes, N. Daskalakis, C.V. Ioannou, The - not so - solid 5.5 cm threshold for abdominal aortic aneurysm repair: facts, misinterpretations, and future directions, Front Surg 3 (2016) 1, https://doi.org/10.3389/fsurg.2016.00001.
[55] G. Galyfos, F. Sigala, K. Mpananis, et al., Small abdominal aortic aneurysms: has anything changed so far? Trends Cardiovasc. Med. 30 (8) (Nov 2020) 500–504, https://doi.org/10.1016/j.tcm.2019.11.006.
[56] R.C. Darling, C.R. Messina, D.C. Brewster, L.W. Ottinger, Autopsy study of unoperated abdominal aortic aneurysms. The case for early resection, Circulation 56 (3 Suppl) (Sep 1977) II161–I164.
[57] S.C. Nicholls, J.B. Gardner, M.H. Meissner, H.K. Johansen, Rupture in small abdominal aortic aneurysms, J. Vasc. Surg. 28 (5) (Nov 1998) 884–888, https://doi.org/10.1016/s0741-5214(98)70065-5.
[58] R. Umebayashi, H.A. Uchida, J. Wada, Abdominal aortic aneurysm in aged population, Aging (Albany NY) 10 (12) (Dec 6 2018) 3650–3651, https://doi.org/10.18632/aging.101702.
[59] I. Propanolol Aneurysm Trial, Propranolol for small abdominal aortic aneurysms: results of a randomized trial, J. Vasc. Surg. 35 (1) (Jan 2002) 72–79, https://doi.org/10.1067/mva.2002.121308.
[60] G. Kiru, C. Bicknell, E. Falaschetti, J. Powell, N. Poulter, An evaluation of the effect of an angiotensin-converting enzyme inhibitor on the growth rate of small abdominal aortic aneurysms: a randomised placebo-controlled trial (AARDVARK), Health Technol. Assess. 20 (59) (Jul 2016) 1–180, https://doi.org/10.3310/hta20590.
[61] J.L. Pinchbeck, J.V. Moxon, S.E. Rowbotham, et al., Randomized placebo-controlled trial assessing the effect of 24-week fenofibrate therapy on circulating markers of abdominal aortic aneurysm: outcomes from the FAME -2 trial, J. Am. Heart Assoc. 7 (19) (Oct 2 2018), e009866, https://doi.org/10.1161/JAHA.118.009866.
[62] J.S. Lindholt, M. Bjorck, J.B. Michel, Anti-platelet treatment of middle-sized abdominal aortic aneurysms, Curr. Vasc. Pharmacol. 11 (3) (May 2013) 305–313, https://doi.org/10.2174/1570161111311030005.
[63] N. Fujimura, J. Xiong, E.B. Kettler, et al., Metformin treatment status and abdominal aortic aneurysm disease progression, J. Vasc. Surg. 64 (1) (Jul 2016) 46–54 e8, https://doi.org/10.1016/j.jvs.2016.02.020.
[64] K.L. Kristensen, A. Pottegard, J. Hallas, L.M. Rasmussen, J.S. Lindholt, Metformin treatment does not affect the risk of ruptured abdominal aortic aneurysms, J. Vasc. Surg. 66 (3) (Sep 2017) 768–774 e2, https://doi.org/10.1016/j.jvs.2017.01.070.
[65] M. Rouer, B.H. Xu, H.J. Xuan, et al., Rapamycin limits the growth of established experimental abdominal aortic aneurysms, Eur. J. Vasc. Endovasc. Surg. 47 (5) (May 2014) 493–500, https://doi.org/10.1016/j.ejvs.2014.02.006.
[66] D.Y. Li, A. Busch, H. Jin, et al., H19 induces abdominal aortic aneurysm development and progression, Circulation 138 (15) (Oct 9 2018) 1551–1568, https://doi.org/10.1161/CIRCULATIONAHA.117.032184.
[67] L. Maegdefessel, J. Azuma, R. Toh, et al., MicroRNA-21 blocks abdominal aortic aneurysm development and nicotine-augmented expansion, Sci. Transl. Med. 4 (122) (Feb 22 2012), 122ra22, https://doi.org/10.1126/scitranslmed.3003441.
[68] L. Maegdefessel, J.M. Spin, U. Raaz, et al., miR-24 limits aortic vascular inflammation and murine abdominal aneurysm development, Nat. Commun. 5 (Oct 31 2014) 5214, https://doi.org/10.1038/ncomms6214.
[69] P.Y. Chen, L. Qin, G. Li, et al., Smooth muscle cell reprogramming in aortic aneurysms, Cell Stem Cell 26 (4) (Apr 2 2020) 542–557, https://doi.org/10.1016/j.stem.2020.02.013.
[70] D. Cai, C. Sun, G. Zhang, et al., A novel mechanism underlying inflammatory smooth muscle phenotype in abdominal aortic aneurysm, Circ. Res. 129 (10) (Oct 29 2021) e202–e214, https://doi.org/10.1161/CIRCRESAHA.121.319374.
[71] M. Masuda, S. Miyazaki-Anzai, M. Levi, T.C. Ting, M. Miyazaki, PERK-eIF2alpha-ATF4-CHOP signaling contributes to TNFalpha-induced vascular calcification, J. Am. Heart Assoc. 2 (5) (Sep 5 2013), e000238, https://doi.org/10.1161/JAHA.113.000238.
[72] U.I. Onat, A.D. Yildirim, O. Tufanli, et al., Intercepting the lipid-induced integrated stress response reduces atherosclerosis, J. Am. Coll. Cardiol. 73 (10) (Mar 19 2019) 1149–1169, https://doi.org/10.1016/j.jacc.2018.12.055.
[73] A. Chattopadhyay, C.S. Kwartler, K. Kaw, et al., Cholesterol-induced phenotypic modulation of smooth muscle cells to macrophage/fibroblast-like cells is driven by an unfolded protein response, Arterioscler. Thromb. Vasc. Biol. 41 (1) (Jan 2021) 302–316, https://doi.org/10.1161/atvbaha.120.315164.
[74] A. Chattopadhyay, P. Guan, S. Majumder, et al., Preventing cholesterol-induced perk (protein kinase RNA-like endoplasmic reticulum kinase) signaling in smooth muscle cells blocks atherosclerotic plaque formation, Arterioscler. Thromb. Vasc. Biol. 42 (8) (Aug 2022) 1005–1022, https://doi.org/10.1161/atvbaha.121.317451.
[75] U.I. Onat, A.D. Yildirim, Tufanli Ö, et al., Intercepting the lipid-induced integrated stress response reduces atherosclerosis, J. Am. Coll. Cardiol. 73 (10) (Mar 19 2019) 1149–1169, https://doi.org/10.1016/j.jacc.2018.12.055.
[76] X.Q. Ni, W.W. Lu, J.S. Zhang, et al., Inhibition of endoplasmic reticulum stress by intermedin1-53 attenuates angiotensin II-induced abdominal aortic aneurysm in ApoE KO Mice, Endocrine 62 (1) (Oct 2018) 90–106, https://doi.org/10.1007/s12020-018-1657-6.
[77] Y. Qin, Y. Wang, O. Liu, et al., Tauroursodeoxycholic acid attenuates angiotensin II induced abdominal aortic aneurysm formation in apolipoprotein E-deficient mice by inhibiting endoplasmic reticulum stress, Eur. J. Vasc. Endovasc. Surg. 53 (3) (Mar 2017) 337–345, https://doi.org/10.1016/j.ejvs.2016.10.026.
[78] C. Li, Q. Fan, H. Quan, M. Nie, Y. Luo, L. Wang, The three branches of the unfolded protein response exhibit differential significance in breast cancer growth and stemness, Exp. Cell Res. 367 (2) (Jun 15 2018) 170–185, https://doi.org/10.1016/j.yexcr.2018.03.033.
[79] G. Zhao, Y. Fu, Z. Cai, et al., Unspliced XBP1 confers VSMC homeostasis and prevents aortic aneurysm formation via FoxO4 interaction, Circ. Res. 121 (12) (Dec 8 2017) 1331–1345, https://doi.org/10.1161/CIRCRESAHA.117.311450.
[80] J.A. Moreno, M. Halliday, C. Molloy, et al., Oral treatment targeting the unfolded protein response prevents neurodegeneration and clinical disease in prion-infected mice, Sci. Transl. Med. 5 (206) (Oct 9 2013), 206ra138, https://doi.org/10.1126/scitranslmed.3006767.
[81] A.M. Flores, J. Ye, K.U. Jarr, N. Hosseini-Nassab, B.R. Smith, N.J. Leeper, Nanoparticle therapy for vascular diseases, Arterioscler. Thromb. Vasc. Biol. 39 (4) (Apr 2019) 635–646, https://doi.org/10.1161/ATVBAHA.118.311569.
[82] C.M. Hu, R.H. Fang, K.C. Wang, et al., Nanoparticle biointerfacing by platelet membrane cloaking, Nature 526 (7571) (Oct 1 2015) 118–121, https://doi.org/10.1038/nature15373.
[83] B. Wang, G. Chen, G. Urabe, et al., A paradigm of endothelium-protective and stent-free anti-restenotic therapy using biomimetic nanoclusters, Biomaterials 178 (Sep 2018) 293–301, https://doi.org/10.1016/j.biomaterials.2018.06.025.
[84] Y. Zhao, R. Xie, N. Yodsanit, M. Ye, Y. Wang, S. Gong, Biomimetic fibrin-targeted and H2O2-responsive nanocarriers for thrombus therapy, Nano Today (Dec 2020) 35doi, https://doi.org/10.1016/j.nantod.2020.100986.
[85] Y. Zhao, T. Shirasu, N. Yodsanit, et al., Biomimetic, ROS-detonable nanoclusters - a multimodal nanoplatform for anti-restenotic therapy, J. Contr. Release 338 (Oct 10 2021) 295–306, https://doi.org/10.1016/j.jconrel.2021.08.025.
[86] Y. Zhao, R. Xie, N. Yodsanit, et al., Hydrogen peroxide-responsive platelet membrane-coated nanoparticles for thrombus therapy, Biomater. Sci. 9 (7) (Apr 7 2021) 2696–2708, https://doi.org/10.1039/d0bm02125c.
[87] J. Cheng, R. Zhang, C. Li, et al., A targeting nanotherapy for abdominal aortic aneurysms, J. Am. Coll. Cardiol. 72 (21) (Nov 27 2018) 2591–2605, https://doi.org/10.1016/j.jacc.2018.08.2188.
[88] H. Wu, C. Xie, R. Wang, J. Cheng, Q. Xu, H. Zhao, Comparative analysis of thoracic and abdominal aortic aneurysms across the segment and species at the single-cell level, Front. Pharmacol. 13 (2022), 1095757, https://doi.org/10.3389/fphar.2022.1095757.
[89] G. Zhao, H. Lu, Z. Chang, et al., Single-cell RNA sequencing reveals the cellular heterogeneity of aneurysmal infrarenal abdominal aorta, Cardiovasc. Res. 117 (5) (Apr 23 2021) 1402–1416, https://doi.org/10.1093/cvr/cvaa214.